Aircraft type recognition in satellite images

J.-W. Hsieh, J.-M. Chen, C.-H. Chuang and K.-C. Fan

Abstract: This paper proposes a hierarchical classification algorithm to accurately recognise aircrafts in satellite images. Since each aircraft in satellite images is captured far from the ground, it has a very small size and often includes various textures, orientations, dazzle paints, and even noise. All of these will present many challenges in extracting useful features and result in unstableness and inaccuracy of aircraft type recognition. Therefore, before recognition, a novel symmetry-based algorithm is proposed to estimate an aircraft's optimal orientation for rotation correction. In addition, several image preprocessing techniques such as noise removal, binarisation, and geometrical adjustments are also applied to removing the above variations. Then, distinguishable features are derived from each aircraft for aircraft recognition. However, different features have different discrimination abilities to recognise the types of aircrafts. Therefore, a novel booting algorithm is proposed to learn a set of proper weights from training samples for feature integration. Owing to this integration, significant improvements in terms of recognition accuracy and robustness can be achieved. Last, a hierarchical recognition scheme is proposed to recognise the types of aircrafts by using the area feature first for a rough categorisation on which detailed classifications are then achieved using several suggested features. Experiments were conducted on a wide variety of satellite images. Experimental results reveal the feasibility and validity of the proposed approach in recognising aircrafts in satellite images.

1 Introduction

Satellite images can be captured without any constraints by time, weather, country boundary, and other environmental factors. Owing to this advantage, there have been many researchers who devoted themselves to utilising satellite images for developing different applications like water and climate observation, land cover classification, energy exploration, etc. Especially, surveillance through satellite images is another important application for military needs and environment protection. Therefore, in the literature [1–5], there have been many different detection schemes proposed for detecting various targets from satellite images such as bridges, airports, roads, streets, buildings, etc. For example, Nevatia and Babu [1] proposed a line edge detector to detect all line-like structures. Gruen and Li [2] used wavelet transforms to sharpen road boundaries. In addition, Geman and Jedynak [3] used an active testing strategy to detect all 1-D line structures as a base to find major roads. Moreover, Shi and Zhu [4] proposed a line matching method to extract road networks from high-resolution satellite images. In addition to line detection, Pesaresi and Benediktsson [5] used several morphological operations and the technique of multi-scale analysis to segment different buildings from satellite images. However, since the objects in satellite images are very small, all the above methods focus only on detecting objects and do not further recognise these objects. For recognising objects, in the past, there have been many methods [6–11] proposed for this task and requiring that the targets should be large enough for feature extraction. For example, Reeves *et al.* [6] and Wallace *et al.* [7] proposed procedures to identify a 3-D object from 2-D images using moments and Fourier descriptors. In addition, Tien and Chai [8] utilised the characteristics of non-uniform rational *B*-splines and cross-ratios to recognise aircraft in images. Greenberg and Guterman [9] used multi-layer neural networks to recognise different targets from aerial images according to the features of Zernike moments. Moreover, Moldovan and Wu [11] used a symbolic approach to recognise hierarchically aeroplanes if all features of an aeroplane were well extracted. However, when recognising the targets in satellite images, all these methods will fail to work since the analysed targets are very small and polluted by different dazzle paints, shadows, and other noise.

In this paper, we propose a novel recognition system for recognising various aircraft in satellite images using a hierarchical boosting algorithm. Since each aircraft in satellite images has different orientations, sizes, textures, and even dazzle paints, before recognition, image pre-processing techniques are first employed to reducing all the above variations to a minimum. The preprocessing tasks include image quality enhancement, noise removal, automatic binarisation, and the adjustments of aircraft scaling and translation. For rotation correction, we propose a novel method to use the symmetrical property of an aircraft to estimate its optimal orientation. In the past, the common method to estimate an object's orientation was through a moment-based analysis [12]. However, an aircraft may have longer wings, shadows, fragments, and other noise. All these factors will make the moment-based method fail to normalise an aircraft having a correct orientation. However, for an aircraft that has been fragmented, polluted,

IEE Proceedings online no. 20059020

doi: 10.1049/ip-vis:20059020

Paper first received 15th March and in revised form 25th November 2004

J.-W. Hsieh is with the Department of Electrical Engineering, Yuan Ze University, 135 Yuan-Tung Road, Chung-Li 320, Taiwan

J.-M. Chen, C.-H. Chuang and K.-C. Fan are with the Department of Computer Engineering, National Central University, Jung-Da Rd., Chung-Li 320, Taiwan

E-mail: shieh@saturn.yzu.edu.tw

and occluded by shadows or noise, its symmetry still maintains. Thus, the symmetry-based method can perform more robustly, effectively, and accurately to correct the orientation of an aircraft than the moment-based method. Then, distinguishable features derived from the characteristics exhibited by aircraft are extracted for aircraft recognition. Four features are used here and derived, respectively, from wavelet transform, Zernike moment, distance transform, and the bitmap itself. Different features have different discrimination abilities to classify aircrafts. In order to integrate these features together, a novel learning scheme is proposed to determine suitable weights from training samples for improving the accuracy of aircraft recognition. Based on these two ingredients, i.e. weights and features, all input aircraft can be recognised very accurately. From experimental results, the proposed method indeed achieves great improvements in terms of accuracy, robustness, and effectiveness in recognising aircraft in satellite images.

2 Overview of the proposed system

This paper proposes a novel system to recognise aircraft in satellite images for military needs. The proposed system can be divided into three modules, i.e. preprocessing, feature extraction, and recognition. Each module is described as follows:

2.1 Preprocessing

Input of the proposed system is an aircraft image captured by a manual or automatic method. Owing to its various appearances in satellite images including changes of orientation, size, position, and textures, a preprocessing module should be first applied for removing out all these unexpected variations. The tasks of preprocessing include binarisation, noise removing, size normalisation, and orientation correction. All the preprocessing tasks are list in Fig. 1.

2.2 Feature extraction

After preprocessing, each aircraft will have the same orientation and similar size. Then, four features are extracted from it for representing its characteristics. The features we used include contours, moments, wavelet coefficients, and original bitmaps. Based on these features, any input aircrafts can be classified well and recognised.

2.3 Aircraft recognition

Different features have different performances to recognise aircraft. In order to get the optimal performance of recognition, these features should be combined together further using a set of proper weights. In this paper, a hierarchical boosting algorithm is proposed to automatically determine the set of weights for feature integration such that different aircrafts can be more accurately recognised. Figure 2 shows details of the proposed recogniser.

In what follows, details of all the preprocessing modules are described in Section 3. Then, details of feature extraction are described in Section 4. Section 5 describes the details of aircraft recognition. After that, in Section 6, some experimental results will be reported to prove the superiority of our proposed algorithm.

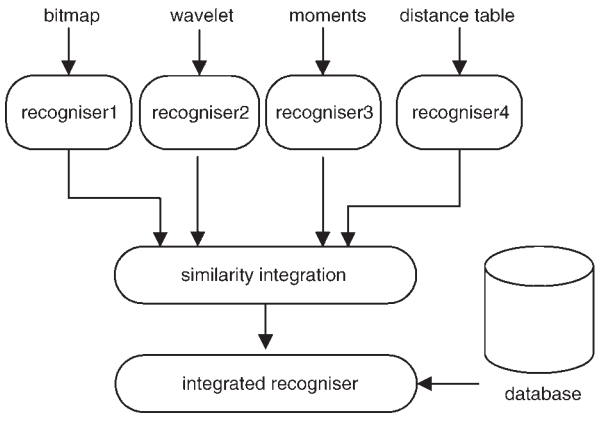

Fig. 2 *Details of proposed recogniser*

3 Preprocessing

Before recognition, each aircraft in a satellite image would be polluted by noise and has different orientations, sizes, and textures. Therefore, image preprocessing techniques such as binarisation, orientation adjustment, and noise removing should be first applied to overcoming these variations. In what follows, details of these techniques are described.

3.1 Binarisation and noise removing

In this paper, a 'minimum within-group variance' dynamic thresholding method [12] is applied to binarising each input region. Figure 3 shows an example of automatic binarisation using this algorithm. After binarisation, a conventional labelling technique is then applied to locate each connected component from the binarised aircraft image. For each connected region, if its size is less than a threshold, it will be considered as noise and then filtered out.

3.2 Orientation estimation and normalisation

In practice, each aircraft will have different orientations when it appears in satellite images In order to recognise this aircraft more accurately and robustly, it should be normalised to a fixed orientation, i.e. the northern direction. In this Section, two methods, the moment-based method and the symmetry-based method, are described for estimating an

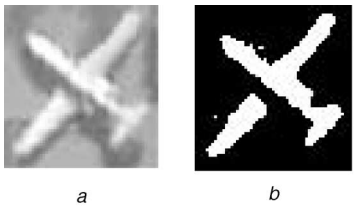

Fig. 3 *Original image and result after binarisation*

a Original aircraft image
b Result after binarisation

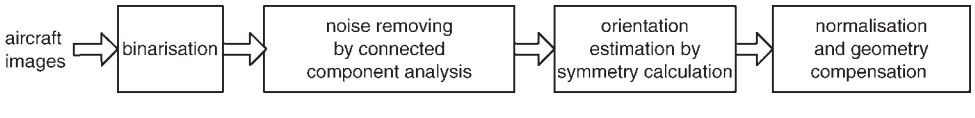

Fig. 1 *Details of preprocessing stage*

optimal orientation of an aircraft for this normalisation. The former method is simpler and more efficient than the latter. However, when noise exists, the symmetry-based method works more robustly and effectively than the former one. In what follows, details of the moment-based method are first described and then the symmetry-based one is proposed.

3.2.1 Orientation estimation by moments: Given a 2-D binary aircraft region $R(x,y)$, the central moments of R can be defined as:

$$(\mu_{p,q})_R = \sum_{(x,y)\in R} (x-\bar{x})^p (y-\bar{y})^q \tag{1}$$

where

$$(\bar{x},\bar{y}) = \left(\frac{1}{|R|}\sum_{(x,y)\in R} x, \frac{1}{|R|}\sum_{(x,y)\in R} y \right)$$

and $|R|$ is the area of R. Here, if a pixel (x,y) belongs to R, the value of $R(x,y)$ is one; otherwise, its value is zero. Then, as shown in Fig. 4, the orientation θ_R of R can be obtained as follows:

$$\theta_R = \arg \min_{\theta} \sum_{(x,y)\in R} [(x-\bar{x})\sin\theta - (y-\bar{y})\cos\theta]^2 \tag{2}$$

Setting the term

$$\frac{1}{\partial\theta}\sum_{(x,y)\in R} [(x-\bar{x})\sin\theta - (y-\bar{y})\cos\theta]^2$$

to zero, we can get

$$\theta_R = \frac{1}{2}\tan^{-1}\left[\frac{2\mu_{1,1}}{\mu_{2,0}-\mu_{0,2}}\right] \tag{3}$$

Then, according to (3), the orientation of R can be obtained. However, like Fig. 5*a*, when an aircraft has two longer wings, the solution in (3) will not be the correct one for orientation normalisation. In addition, if noise exists (Fig. 5*b*), (3) will fail to find a correct solution for the orientation normalisation. In what follows, a symmetry-based method will be proposed for this orientation adjustment.

3.2.2 Orientation estimation through symmetry comparison: In practice, each aircraft will have a pair of symmetrical wings for maintaining stability when it flies. Therefore, all aircraft are symmetrical about their body axis. Even though they are polluted by noise or have longer wings, this symmetry is still kept. Therefore, in

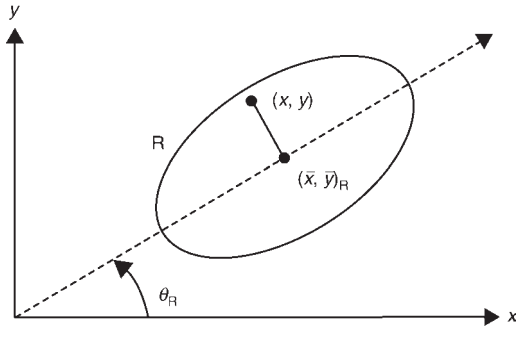

Fig. 4 *Gravity centre $(\bar{x},\bar{y})_R$ and orientation θ_R of the object R*

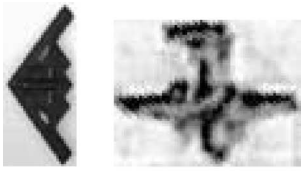

Fig. 5 *Aircraft have different appearances and orientations*
a Aircraft with longer wings
b Aircraft with noise

what follows, we will present a symmetry-based method to find the optimal direction of an aircraft for the orientation normalisation.

Let the symmetry of an aircraft R be measured by $\Phi(R)$. If θ_{axis} is the direction of the body axis of R, it should satisfy the following equation:

$$\theta_{axis} = \arg \max_{0^\circ \le \theta < 180^\circ} \Phi(R^\theta) \tag{4}$$

where R^θ is the rotated version of R obtained by rotating R with an angle θ. In this equation, two directions with 180° difference are considered the same. To solve (4), the first step is to define the symmetry measure $\Phi(R)$. Let $H_R(j)$ be the horizontal projection of R at the jth position along the x direction, i.e.

$$H_R(j) = \sum_{0\le i < w_R} R(i,j) \tag{5}$$

where w_R is the width of R. According to (5), the central x coordinate of the jth row in R can be obtained as follows:

$$x_R(j) = \frac{1}{H_R(j)}\sum_{0\le i < w} i \times R(i,j) \tag{6}$$

As shown in Fig. 6, the black line in Fig. 6*b* is drawn according to the central x coordinates of all rows extracted from Fig. 6*a*. Clearly, if R is toward the northern direction, the black line is the body axis of R and all the values $\{x_R(j)\}$ are similar. Thus, the variance of $\{x_R(j)\}$ can be used as a good index to measure the symmetry of R. Let X_R be the set of all the central x co-ordinates, i.e. $X_R = \{x_R(j)\}_{0\le j < h_R}$. The variance of X_R can be defined as:

$$\sigma_X(R) = \sqrt{\frac{1}{|X_R|}\sum_{x\in X_R}(x-\bar{x})^2}, \tag{7}$$

where $\bar{x}$ is the mean of X_R and $|X_R|$ the number of elements in X_R. Then, (4) can be rewritten as follows:

$$\theta_{axis} = \arg \min_{0^\circ \le \theta < 180^\circ} \sigma_X(R^\theta) \tag{8}$$

However, it is very time-consuming to solve (8) since there are too many rotation calculations required for solving (8). To tackle this problem, we propose a coarse-to-fine approach to solving (8) more efficiently. At the coarse stage, the range of possible orientation angles is quantised into a smaller set with a large quantisation step, for example,

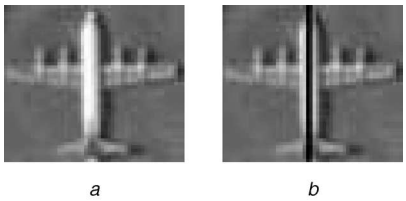

Fig. 6 *Aircraft with northern direction*
a Original aircraft
b Black line is direction of *a*

20°. Then, at the fine stage, a smaller quantisation step is gradually used for finding the optimal rotation angle. In what follows, details of our proposed symmetry-based rotation estimation algorithm are described.

Symmetry-based orientation estimation algorithm:

Input: a binary aircraft region R.

Output: the major orientation θ_{axis} of R.

Step 1: Let $s = 20$ and $\Theta = \{i \times s \,|\, i = 0, 1, \ldots, (180)/(s)\}$. Let Φ = NULL.

Step 2: For each θ in Θ, calculate the symmetry measure $\sigma_X(R^\theta)$ according to (7).

Step 3: Sort all angles θ in an ascendant order according to the value of $\sigma_X(R^\theta)$.

Step 4: If $s = 1$, choose the θ with the smallest $\sigma_X(R^\theta)$ as the desired solution θ_{axis} and go to Step 8. Otherwise, collect the top N angles θ with smaller $\sigma_X(R^\theta)$ from Θ to the set Φ as possible candidates, where $N = 1 + |\Theta|/8$ and $|\Theta|$ is the number of elements in Θ.

Step 5: Half the quantisation step, i.e., $s = s/2$. Let $\Phi' =$ NULL.

Step 6: For each element ϕ in Φ, generate two new candidates $\beta + s$ and $\beta - s$ to the new set Φ'.

Step 7: $\Theta = \Phi \cup \Phi'$. Let $\Phi =$ NULL. Go to Step 2.

Step 8: Return the θ_{axis} as the desired solution.

Table 1 shows the performance comparisons between the moment-based method and the symmetry-based one. Clearly, when robustness is considered, the proposed symmetry-based method is better for being chosen. Since the size of an aircrafts is small, the rotation adjustment can be performed very efficiently.

Alternatively, although the proposed symmetry-based method can accurately estimate the orientation of an aircraft's axis, there would be 180° orientation difference between this axis and the actual orientation of an aircraft. For example, in Fig. 7*a*, the orientation of this aircraft is towards to the south. However, the major axis of this aircraft we estimate is towards to the north. This problem can be tackled easily by judging the area of this aircraft head. In practice, the head of an aircraft will occupy a smaller area than its tail. Therefore, for an aircraft region, if its head is toward the north, its upper part should occupy less area than its lower part. Figure 8 shows the results of aircraft after orientation adjustment.

Table 1: Comparisons between the moment-based method and the symmetry-based method

Methods Items	Moment-based	Symmetry-based
Speed	*	
Robustness		*
Multiple axis		*
Kinds of image	Images with longer body axis	symmetrical Images

a *b* *c*

Fig. 7 *Result of judgment on aircraft's head and tail*

a Original image
b Head occupies less area than tail
c Result of rotation

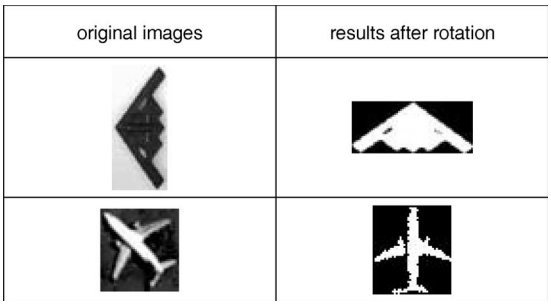

Fig. 8 *Aircraft after orientation estimation and adjustment*

3.3 Size normalisation

In addition to an orientation adjustment, before feature extraction, the size and centre of each processed aircraft also require normalising to a regular size and the original, respectively. In this paper, the regular size is defined as 24×32.

4 Feature extraction

This paper uses four features to describe the characteristics of an aircraft Some feature is used for describing its inner properties and some feature is used for its outer properties. The four features include binary map, contours, moments, and wavelet coefficients, respectively. Other features like the ratio between the lengths of wings and body axis are also good for aircraft recognition. However, the 'ratio' is easily affected by shadows and noise and thus not considered here. In what follows, details of each feature are introduced.

4.1 Binary map

Owing to the nature of satellite images, the size of an aircraft captured from satellites is not large enough for feature extraction. Therefore, the raw binary map is a good candidate of feature for aircraft recognition. In our representation, 0 is used for representing the background and 1 for the foreground. Assume Map_Q and Map_F are the binary maps of a query aircraft Q and one aircraft F in the database, respectively. The distance between Map_Q and Map_F can be defined as follows:

$$d_{Map}(Q,F) = \sum_{0 \le i < w_Q} \sum_{0 \le j < h_Q} |Map_Q(i,j) - Map_F(i,j)| \quad (9)$$

where w_Q and h_Q are the width and height of Q, respectively.

4.2 Aircraft contour

Contour is also a good feature to describe an aircraft. Traditionally, the common technique used for contour representation is chain coding. However, this technique is affected easily by noise. Therefore, different from chain coding, this paper uses a distance transform to convert an object boundary to a distance map. Based on this map, different aircrafts can be discriminated well.

First, a 3×3 mask is used to detect all boundary points from an aircraft image. When this mask is used and moved at a non-zero pixel p, if one pixel in this mask is zero, then p is a boundary pixel. Figure 9*b* shows the result of boundary detection of Fig. 9*a*. Assume B_A is a set of boundary pixels extracted from an aircraft A. Then, the distance transform of a pixel p in A is defined as.

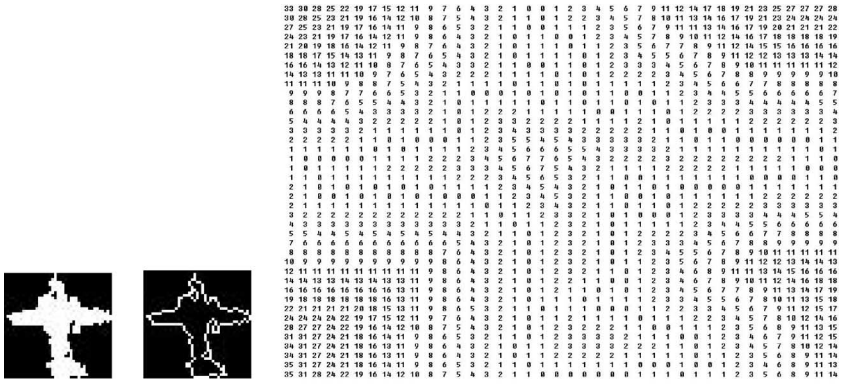

a b c

Fig. 9 *Result of distance transform*

a Original image
b Boundaries of *a*
c Distance transform of *b*

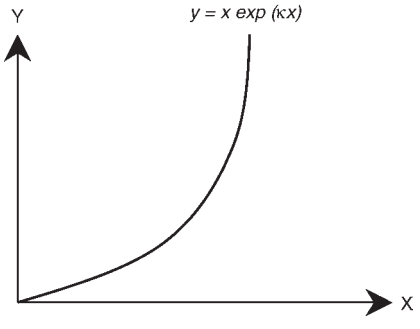

Fig. 10 *Value of y is increased nonlinearly when x increases*

$$DT_A(p) = \min_{q \in B_A} d(p,q) \tag{10}$$

where $d(p,q)$ is the Euclidian distance between p and q. In order to enhance the strength of distance changes, (10) is further modified as follows.

$$\overline{DT}_A(p) = \min_{q \in B_A} d(p,q) \times \exp(\kappa d(p,q)) \tag{11}$$

where $\kappa = 0.1$. Like Fig. 10, when x increases more, the value of y will increase more rapidly than x. Figure 9*c* shows the result of the distance transform of Fig. 9*b*. Then, the distance of distance maps between Q and F is defined as:

$$d_C(Q,F) = \frac{1}{|F|} \sum_{r \in B_F} |\overline{DT}_Q(r) - \overline{DT}_F(r)| \tag{12}$$

where $|F|$ is the image size of F.

4.3 Zernike moments

Zernike moments can provide good properties of size, translation, and rotation invariances for shape descriptions. Thus, this representation technique has been applied successfully to many applications [13–15], including OCR, trademark retrieval, traffic mark detection, and so on. Let $V_{pq}(x,y)$ be a Zernike basis polynomial with p order and q repetition, i.e.

$$V_{pq}(x,y) = R_{pq}(\rho) \exp(jq\theta) \tag{13}$$

where $p \geqq 0$, $|q| \leqq p$, $p - |q|$ is even, $x^2 + y^2 \leqq 1$, $\rho = \sqrt{x^2 + y^2}$, $\theta = \arctan(y/x)$, and $R_{pq}(\rho)$ is defined as:

$$R_{pq}(\rho) = \sum_{l=0}^{(p-|q|)/2} (-1)^l \frac{(p-l)!}{l!\left(\frac{p+|q|}{2} - l\right)!\left(\frac{p-|q|}{2} - l\right)!} \rho^{p-2l}. \tag{14}$$

Then, given an image $f(x,y)$, its Zernike moment with p order and q repetition is defined as:

$$A_{pq} = \frac{n+1}{\pi} \sum_{x^2+y^2 \leq 1} f(x,y) V^*_{pq}(x,y), \tag{15}$$

where $V^*_{pq}(x,y)$ is the conjugate complex of $V_{pq}(x,y)$. If $f^\alpha(x,y)$ is the version of $f(x, y)$ after rotating α angle, then:

$$\begin{aligned} A^\alpha_{pq} &= \frac{n+1}{\pi} \sum_{x^2+y^2 \leq 1} f^\alpha(x,y) V^*_{pq}(x,y) \\ &= A_{pq} \exp(-jq\alpha) \end{aligned} \tag{16}$$

Since $\|A^\alpha_{pq}\| = \|A_{pq}\|$, the absolute version of A_{pq} is rotationally invariant. In addition, if A_{pq} is calculated according to the centre of $f(x,y)$, it is also transition invariant. Moreover, A_{pq} is also scaling-invariant if it is further normalised by $\|A_{00}\|$, i.e. $ZM_{pq} = \|A_{pq}\|/\|A_{00}\|$. When calculating the Zernike moments, we require that the order $p \leq 9$ and thus 29 moment features are extracted from an aircraft image. Assume that $ZM_{pq}(Q)$ and $ZM_{pq}(F)$ represent the Zernike moments of a query aircraft Q and a aircraft F in the database, respectively. Then, the distance of Zernike moments between Q and F can be defined as:

$$d_{ZM}(Q,F) = \sum_{0 < p \leq 9, |q| \leq p, p-|q| \text{is even}} |ZM_{pq}(Q) - ZM_{pq}(Q)|. \tag{17}$$

4.4 Wavelet coefficients

Wavelet transform is a very useful tool to represent images at different resolutions. It has been applied successfully in many applications like compression, watermarking, texture analysis, communications, etc. The wavelet transform uses two kinds of filers to decompose a signal into different resolutions, i.e., the lowpass filter $h(k)$ and the highpass one $g(k)$. Then, given a discrete signal $f(n)$ (assumed at the fine resolution $j = 0$ and represented as $S_0 f(n)$), with the lowpass filter $h(k)$, the approximation of $f(n)$ at lower resolution j-1 can be calculated as follows:

$$S_{j-1}f(n) = \sum_{k=-\infty}^{\infty} S_j f(k)h(k-2n) \tag{18}$$

In addition, information content lost between $S_j f(n)$ and $S_{j-1}f(n)$ can be obtained using the highpass filter $g(k)$ as follows:

$$W_{j-1}f(n) = \sum_{k=-\infty}^{\infty} S_j f(k)g(k-2n) \tag{19}$$

From the view of signal processing, $S_{j-1}f(n)$ and $W_{j-1}f(n)$ are, respectively, the components of low frequency and high frequency of $S_j f(n)$. The above procedure, which is also known as the subband coding, can be performed repeatedly. Figure 11*a* shows the diagram of 1-D wavelet transform. The 1-D wavelet transform can be extended easily to two dimensions. The simplest way to generate 2-D wavelet transform is to apply two 1-D transforms to the rows and columns of a 2-D signal $f(m, n)$, respectively. Figure 11*b* shows the block diagram of a 2-D wavelet transform. Given $f(m, n)$, convolving its rows with $h(k)$ and $g(k)$, we get two sub-images whose horizontal resolutions are reduced by a factor of 2. Both sub-images are then filtered columnwise and downsampled to yield four quarter-size output sub-images. Figure 12 shows the result of three-scale wavelet transform. Here, the filters $h(k)$ and $g(k)$ we use are the D4 family of Daubeches's basis, i.e. $h(0), h(1), h(2), h(3)\} = \left\{\frac{1+\sqrt{3}}{4\sqrt{2}}, \frac{3+\sqrt{3}}{4\sqrt{2}}, \frac{3-\sqrt{3}}{4\sqrt{2}}, \frac{1-\sqrt{3}}{4\sqrt{2}}\right\}$ and $\{g(0), g(1), g(2), g(3)\} = \{h(3), -h(2), h(1), -h(0)\}$.

In this paper, a three-scale wavelet transform is used to process all aircraft images. Then, each wavelet coefficient is quantised to three levels, i.e. 1, 0, −1, if its value is larger than 0, equal to 0, and less than 0, respectively. Figure 12*c* shows the quantised result of Fig. 12*b*. Clearly, the shape of this aircraft is still kept. After that, all the quantised coefficients are recorded for further recognition. When recording, each wavelet coefficient is furtehr classified into different bands, i.e., *LL*, *LH*, *HL*, and *HH*. According to this classification, p is labelled as 1, 2, 2, and 4 if it locates in the *LL*, *LH*, *HL*, *HH* bands, respectively. Thus, the distance of wavelet coefficients between Q and F can be defined as:

$$d_W(Q,F) = \sum_p l(p)\left|Coeff_F^W(p) - Coeff_Q^W(p)\right| \tag{20}$$

where $Coeff_Q^W(p)$ and $Coeff_F^W(p)$ are, respectively, the coefficients of wavelet transforms of Q and F at the point p, and $l(p)$ is the labelling vale of p.

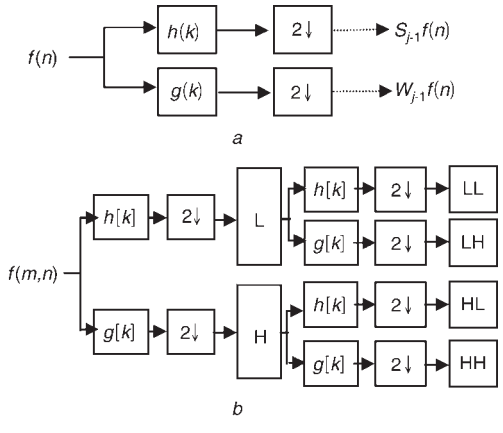

Fig. 11 *Block diagram of discrete wavelet transform*
a 1-D wavelet transform
b 2-D wavelet transform

Fig. 12 *Result of three-scale wavelet transform*
a Original image
b Result of 2-D wavelet transform
c Quantised result of *b*

5 Feature integration and comparisons

In this paper, four features are used to describe the characteristics of an aircraft. For recognition, these different features should be integrated together. In Section 4, we have presented different distance measures for comparing these features between different aircraft. However, these measures have different magnitudes and effects in aircraft recognition. Therefore, in what follows, a normalisation scheme is first described and then a novel learning algorithm is proposed to learn proper weights from training data for feature integration and aircraft recognition.

5.1 Recognition with one single feature

Let $d(Q,F)$ denote a distance measure of one feature between a query aircraft Q and an aircraft F in the database. For all aircraft F_i, we can sort them in an ascendant order according to the measure $d(Q,F_i)$. Based on the sorted result, a normalisation scheme can be proposed to recalculate the distance between Q and F_i. Then, a voting technique is proposed to improve the accuracy when recognising Q. In the result, each element F_i with a lower value of $d(Q,F_i)$ will have a lower index $Idx(F_i)$. Assume that the database has L elements. Then, each element F_i in the database is assigned to a new score for normalisation using the rule:

$$Score_Q(F_i) = 1 - \frac{Idx(F_i)}{L} \tag{21}$$

where the highest score, 1, is assigned to the top one and the score is gradually decreased to 0 according to the value $Idx(F_i)$. Assume there are K categories of aircraft in the database, where each class C_k has N_{C_k} samples. Then, the similarity between Q and C_k can be calculated as follows:

$$S(Q,C_k) = \frac{1}{N_{C_k}} \sum_{F_i \in C_k} Score_Q(F_i) \tag{22}$$

Based on (22), the proposed system classifies the Q into class l when:

$$\forall k \neq l,\ S(Q,C_l) \geq S(Q,C_k) \tag{23}$$

In (23), the actual form of $d(Q,F_i)$ is not specifically defined. The $d(Q,F_i)$ can be replaced accordingly by (9), (12), (17), and (20) if the feature used is binary map, contours, moments, and wavelet coefficients, respectively.

5.2 Recognition with multiple features

In Section 5.1, a method has been described to recognise an aircraft based on only one feature. Assume $S_i(Q,C_k)$ is a similarity between Q and a category C_k based on the ith

feature. When considering all the used features, the integrated similarity between Q and C_k can be represented by a linear combination of all similarities $S_i(Q, C_k)$ as:

$$S_{\text{integration}}(Q, C_k) = \sum_{i=0}^{N_f-1} w_i S_i(Q, C_k) \tag{24}$$

where w_i is a weight for balancing the contribution of $S_i(Q, C_k)$ and N_f the number of features used in this formulation. In this paper, we propose a novel learning algorithm to learn the weight w_i from training samples based on a boosting concept. Assume U is the set of training samples, where U^k is a subset of U whose elements belong to the category C_k. Then, given a sample u_j^k in the training set U^k, the proposed learning algorithm increase the weight w_i if the ith feature lets one instance in C^k have the best ranking. After examining all training samples in U several times, the weights $\{w_i\}$ will gradually converge and thus the optimal solution of $\{w_i\}$ can be obtained. In what follows, details of the proposed learnin algorithm are described.

Weight learning algorithm

Input: MaxIterations=10;

Step 1: Set all the values of $\{w_i\}_{i=0,\ldots,N_f-1}$ to be $1/N_f$.

Step 2: Let $t = 0$ and $\bar{w}_i = w_i$ for $i = 1, \ldots, N_f - 1$.

Step 3: For each sample u_j in U,

3.1 For $i = 0$ to $N_f - 1$

3.1.1 Calculate $S_i(u_j, C_n)$ for all categories, where $n = 1, \ldots, K$.

3.1.2 Sort all categories C_n in decendant order according to the similarity $S_i(u_j, C_n)$.

3.1.3 Get the sorted index $Index_j(i)$ of the category which u_j beglongs to.

3.2 $l = \arg \min_{0 \leqslant i < N_f} Index_j(i)$.

3.3 Update the weight of the lth feature as follows: $w_l = w_l + \Delta w$, where $\Delta w = 0.01$.

3.4 Normalise w_i by $(w_i)/\left(\sum_{i=0}^{N_f-1} w_i\right)$ for all i.

Step 4: $\varepsilon = (1)/(N_f) \sum_{i=0}^{N_f-1} (w_i - \bar{w}_i)^2$ and $t = t + 1$.

Step 5: If $\varepsilon = 0$ or $t <$ MaxIterations, go to Step 2. Otherwise, the set of desired weights $\{w_i\}_{i=0,\ldots,N_f-1}$ is obtained.

With the weights $\{w_i\}_{i=0,\ldots,N_f-1}$ and (24), the similarity between Q and one specific category C_k can be accurately estimated. Then, when multiple features are used, the proposed system classifies Q into the class l if

$$S_{\text{integration}}(Q, C_l) \geq S_{\text{integration}}(Q, C_k) \text{ for } \forall k \neq l. \tag{25}$$

5.3 Hierarchical classification

In Section 5.2, four features are used for aircraft recognition. However, the area of an aircraft is also an important feature for this recognition task. Assume U is the database that includes all training aircrafts for weight training. Using the 'area' feature, U can be classified into two classes, i.e. the one U_{large} having all large aircraft and the one U_{small} with all small aircraft. According to U_{large}, we can get a set of weights $\{w_i^{\text{large}}\}_{i=0,\ldots,N_f-1}$ to construct a similarity measure $S_{\text{integration}}^{\text{large}}(Q, C_i)$ for recognising all large aircraft in details. Similarly, according to U_{small}, the set of weights $\{w_i^{\text{small}}\}_{i=0,\ldots,N_f-1}$ and the measure $S_{\text{integration}}^{\text{small}}(Q, C_i)$ can be constructed for recognizing all small aircrafts. Let C_{small} and C_{large} be the categories of small and large aircrafts, respectively. When recognising a query aircraft Q, the first stage is to classify Q as C_{small} or C_{large} according to the area of Q. If Q belongs to C_{small}, the similarity $S_{\text{integration}}^{\text{small}}(Q, C_i)$ is used for further aircraft recognition. Otherwise, the similarity $S_{\text{integration}}^{\text{large}}(Q, C_i)$ is used for classifying large aircraft in more details. In what follows, details of our hierarchical recognition scheme are described.

Hierarchical recognition algorithm

Input: a query aircraft Q.

Step 1: Classify Q according to the area of Q, i.e.

$$Q \in \begin{cases} C_{\text{small}} & \text{if the area of } Q \text{ is close to } |C_{\text{small}}|; \\ C_{\text{large}}, & \text{otherwise,} \end{cases}$$

where $|C_{\text{small}}|$ is the mean area of all aircrafts in C_{small}.

Step 2: If $Q \in C_{\text{small}}$, recognise Q according to the similarity $S_{\text{integration}}^{\text{small}}(Q, C_k)$. Otherwise, recognise Q according to the measure $S_{\text{integration}}^{\text{large}}(Q, C_k)$.

6 Experimental results

In order to analyse the performance of our proposed approach, a test database containing 218 aircraft, which come from 12 categories, was constructed. In addition, a training database containing 70 aircraft was adopted to train and learn proper weights for increasing the accuracy of aircraft recognition. During recognition, 4 aircraft per each category were used to perform the voting technique (discussed in Section 5.2). Table 2 shows the 12 types of aircrafts built here for recognition. In this Table, each row includes 4 templates for enhancing the robustness and accuracy of recognition. Aircraft at different rows mean that they are from different categories.

For the first set of experiments, we wanted to analyse the performances of the above four features to recognise desired aircrafts. Figure 13 shows the result of querying the 'B2' aircraft when the moment feature was used. Figure 14 shows another query result of the 'A3' aircraft when the feature of wavelet coefficients is used. Table 3 lists the average accuracies of recognition when different features were used. Clearly, the Zernike moments and wavelet coefficients have better discrimination powers. For the second set of experiments, the performance of our method with multiple features was examined. In order to get proper weights for this integration, a set of 70 aircraft was used for training. Table 4 lists the result of weight learning. Clearly, the Zernike moment has a larger weight than other features. Figure 15 shows the recognition results when multiple features were used. Figure 15*a* is the result when an 'A3' aircraft was queried and Fig. 15*b* is the result of 'B4'. The average accuracy of the integration scheme was shown in the *6*th column of Table 3. Clearly, the proposed integration method shows improvement in terms of recognition accuracy, i.e. nearly 18%.

Alternatively, if the resolution of each processed satellite image can be given in advance, the area of aircraft will become a very useful feature in recognising aircrafts. Thus, the proposed hierarchical classification scheme can be applied for much improving the accuracy of recognition. In this scheme, according to the area feature, all the input aircraft are first classified into two rough categories. Then, other features except the area are used to finely classify these aircrafts. In Table 2, according to the area features, all the aircraft are classified to two rough classes '*S*' and '*L*'. Here, only the four categories B1, B2, B3, and B4 are classified as '*L*'. Other ones are recognised as '*S*'. Then, two sets of proper weights can be trained from the '*S*' and '*L*' categories, respectively. Table 5 lists these trained results of

Table 2: Types of aircraft built in the database

A1				
A2				
A3				
A4				
C1				
C2				
C4				
C5				
B1				
B2				
B3				
B4				

Fig. 13 *Recognition result when 'B2' image was used and the moment feature was adopted*

Fig. 14 *Recognition result of 'C3' aircraft when the feature of wavelet coefficients is used*

feature weights for the '*S*' and '*L*' categories. According to these weights, the proposed hierarchical classification scheme can be then applied to classifying aircraft more accurately. When recognising an unknown aircraft, it is first classified to '*S*' class or '*L*' class according to its area feature. Then, its corresponding similarity measure $S^{\text{small}}_{\text{integration}}(Q, C_k)$ or $S^{\text{large}}_{\text{integration}}(Q, C_k)$ can be selected for classifying it in more details. Table 6 shows the recognition rates of different features when a hierarchical scheme is used. The average recognition accuracy of the hierarchical scheme is high and up to 97.14%, where only six aircraft are wrongly recognised. When examining these errors, there are three '*S*2' aircraft being misclassified as '*L*3'. If the errors in the first stage can be ignored, they still can be classified correctly with our proposed integration scheme. Thus, the average accuracy is up to 98.6%. Three other wrong cases are caused by misclassifying '*L*3' to '*L*4' owing to their similar shapes and shadows. If more representative templates (not only 4 templates) are used to represent an aircraft type, the three failure cases will be tackled well. According to the above experimental results, the superiority of our method has been verified.

Table 3: Types of aircraft built in database

Features					
Rate	Bitmap	Dist table	Z.M.	Wavelets	Integration
Accuracy	68.57%	72.86%	77.14%	77.01%	87.14%

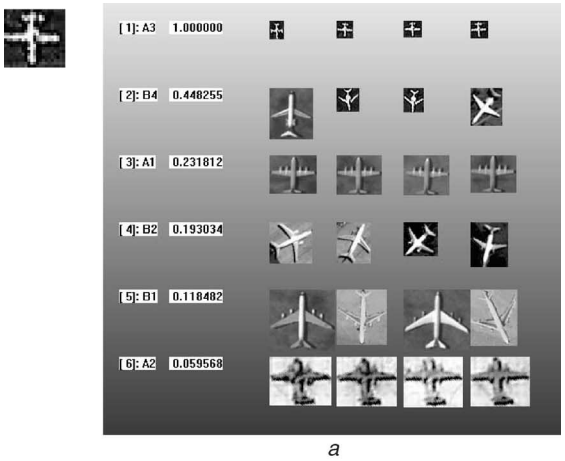

a

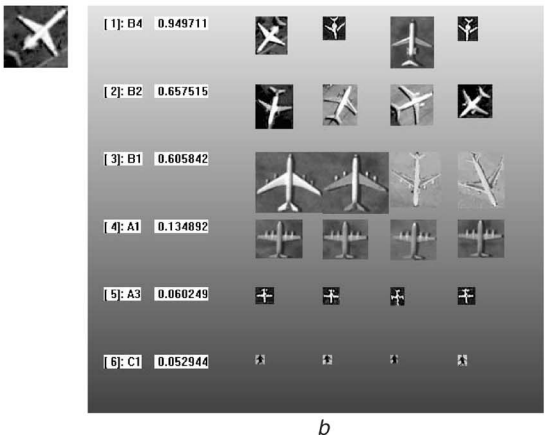

b

Fig. 15 *Recognition results when all features were used*

a Recognition result when '*A*3' aircraft is recognised
b Recognition result when '*B*4' image is input

Table 4: Trained weights of different features

Features	Bitmap	Dist table	Z.M.	Wavelets
Weights	0.230765	0.233395	0.276299	0.259541

Table 5: Trained weights of different features at the '*S*' and '*L*' categories

Features Weights	Bitmap	Dist table	Z.M.	Wavelets
S	0.23588	0.207227	0.306438	0.250455
L	0.202005	0.278931	0.296067	0.222997

Table 6: Recognition accuracies of different features when a hierarchical scheme is used

Features Recognition	Bitmap	Dist table	Z.M.	Wavelets	Integration
Accuracy	89%	92.71%	93.29%	90.43%	97.14%

7 Conclusions

In this paper, we have presented a hierarchical recognition method to recognise types of aircraft from satellite images. At the beginning, the method takes advantages of aircraft symmetry to estimate an aircraft's orientation for rotation adjustment. Then, four features including bitmaps, wavelet coefficients, Zernike moments, and distance maps were used to capture different shape characteristics of an aircraft. Furthermore, a novel learning method was presented to automatically determine a set of proper weights of features from training sets for feature integration. Through analysis, the best method to recognise aircraft is to use the area feature first for roughly categorising aircrafts and then detailed classifications are made according to the suggested four features. The contributions of this paper can be summarised as follows:

(*a*) A symmetry-based method was proposed to estimate an aircraft's optimal orientation. Even though this aircraft has been populated by shadows or noise, the proposed method still can robustly and effectively achieve the rotation adjustment.
(*b*) A hierarchical recognition scheme was proposed to recognise the types of aircraft by incorporating suitable weights into each feature and classifying aircrafts at different levels. The integration has been proved very usefully in aircraft recognition.

Experimental results have proved the superiority of our proposed method.

8 Acknowledgment

This work was supported in part by the National Science Council of Taiwan under Grant NSC92-2213 -E-150-049.

9 References

1 Nevatia, R., and Babu, K.R.: 'Linear feature extraction and description', *Comput. Graph. Image Process.*, 1980, **13**, pp. 257–269
2 Gruen, A., and Li, H.: 'Semi-automatic road extraction by dynamic programming', *Int. Arch. Photogramm. Remote Sens.*, 1994, **30**, (3/1), pp. 324–332
3 Geman, D., and Jedynak, B.: 'An active testing model for tracking roads in satellite images', *IEEE Trans. Pattern Anal. Mach. Intell.*, 1996, **18**, (1), pp. 1–14
4 Shi, W., and Zhu, C.: 'The line segment match method for extracting road network from high-resolution satellite images', *IEEE Trans. Geosci. Remote Sens.*, 2002, **40**, (2), pp. 511–514
5 Pesaresi, M., and Benediktsson, J.A.: 'A new approach for the morphological segmentation of high-resolution satellite imagery', *IEEE Trans. Geosci. Remote Sens.*, 2001, **39**, (2), pp. 309–320
6 Reeves, A.P., Prokop, R.J., Andrews, S.E., and Kuhl, F.P.: 'Three-dimensional shape analysis using moments and Fourier descriptors', *IEEE Trans. Pattern Anal. Mach. Intell.*, 1988, **10**, (6), pp. 937–943
7 Wallace, T.P., and Wintz, P.A.: 'An efficient three-dimensional aircraft recognition algorithm using normalized Fourier descriptors', *Comput. Graph. Image Process.*, 1980, **13**, pp. 99–126
8 Tien, S.C., and Chia, T.L.: 'Using cross-ratios to model curve data for aircraft recognition', *Pattern Recognit. Lett.*, 2003, **12**, pp. 2047–2060
9 Greenberg, and Guterman, J.: 'Neural-network classifiers for automatic real-world aerial image recognition', *Appl. Opt.*, 1996, **35**, (23), pp. 4598–4608
10 Latecki, L., and Lakämper, R.: 'Application of planar shape comparison to object retrieval in image databases', *Pattern Recognit.*, 2002, **35**, (1), pp. 15–29
11 Moldovan, D.I., and Wu, C.I.: 'A hierarchical knowledge based system for airplane classification', *IEEE Trans. Softw. Eng.*, 1998, **14**, (12), pp. 1829–1834
12 Sonka, M., Hlavac, V., and Boyle, R.: 'Image processing, analysis and machine vision' (Chapman & Hall, London, U. K., 1993)
13 Liao, S., and Pawlak, M.: 'Image analysis with Zernike moment descriptors'. 1997 Canadian Conf. on Electrical and Computer Engineering (CCECE), St. John's, May 25–28, 1997, pp. 700–703
14 Liao, S.X., and Pawlak, M.: 'On the accuracy of Zernike moments for image analysis', *IEEE Trans. Pattern Anal. Mach. Intell.*, 1998, **20**, (12), pp. 1358–1364
15 Alferez, R., and Wang, Y.F.: 'Geometric and illumination invariants for object recognition', *IEEE Trans. Pattern Anal. Mach. Intell.*, 1999, **21**, (6), pp. 505–536